Nuclear Instruments and Methods in Physics Research A 382 (1996) 495–502

ELSEVIER

NUCLEAR INSTRUMENTS & METHODS IN PHYSICS RESEARCH Section A

A method for the determination of counting efficiencies in γ-spectrometric measurements with HPGe detectors

J.P. Bolivar[a,*], R. García-Tenorio[b], M. García-León[c]

[a]Dept. Fisica Aplicada, E.P.S. La Rábida, Universidad de Huelva, 21819-Palos, Huelva, Spain
[b]Dept. Fisica Aplicada, ETS Arquitectura, Avda, Reina Mercedes s/n, 41012-Sevilla, Spain
[c]Facultad de Fisica, Universidad de Sevilla, Apdo 1065, 41080-Sevilla, Spain

Received 2 January 1996; revised form received 11 June 1996

Abstract

In this paper a general method for γ-ray efficiency calibration is presented. The method takes into account the differences of densities and counting geometry between the real sample and the calibration sample. It is based on the γ-transmission method and gives the correction factor f as a function of E_γ, the density and counting geometry. Altough developed for soil samples, its underlying working philosophy is useful for any sample whose geometry can be adequately reproduced.

1. Introduction

Generally speaking, γ-ray spectrometry provides a fast, multielemental and non-destructive method of radioactivity measurements which is widely used for studying the presence of radionuclides in nature. Although less sensitive than traditional radiochemical methods, all the above mentioned features make such technique superior to them in many cases [1–4].

In γ-spectrometry the formula for the calculation of the activity concentration, A, of a given radionuclide in a sample of mass (or volume) M is

$$A = \frac{n}{P_\gamma \epsilon M} \tag{1}$$

where n is the net count rate under the full-energy peak corresponding to the photon of energy E_γ emitted by the radionuclide of interest with an emission probability P_γ and M is the mass (or volume) of the sample. The factor ϵ is the full-energy peak efficiency corresponding to E_γ.

The accurate determination of ϵ is the key problem when γ-spectrometry is used for radionuclide measurements. It is, at the same time, the most difficult problem to be successfully solved. As it is known, given a counting geometry, ϵ depends on E_γ, the density and the composition of the sample. Therefore, by obtaining $\epsilon(E_\gamma)$ for a calibration sample, with the same density, ρ, and similar composition as the samples of unknown activities, the problem is solved, since such function $\epsilon(E_\gamma)$ can be confidently used in Eq. (1) to obtain A. This is a very common practice in laboratories engaged in environmental radioactivity determinations, since, in principle, it is an easy task.

However, it is very difficult to obtain calibration samples with identical ρ as the real samples. Furthermore, very frequently it is impossible to prepare calibration samples from real samples since not always one has as much an amount of sample as would be needed [5].

As an alternative, many laboratories when, for instance, measuring soil samples from a given geographical area use one of the soil samples as calibration sample. Nevertheless, this practice, although simple, gives rise to systematic errors in A. Indeed, the obtained $\epsilon(E_\gamma)$ cannot be rigorously applied to all the samples since their densities are not identical [6–8]. Thus, each natural sample has its own $\epsilon(E_\gamma)$, which should be found for each of it.

This is not a realistic approach to the problem of $\epsilon(E_\gamma)$ measurement because it is time consuming and many times impossible to accomplish. In our tackling with the measurement of γ-emitters in soil samples from the Southwest of Spain we have dealt with samples of clearly different ρ. It has induced us to develop a method for ϵ determination which helps to overcome the problems described above. Thus, we present in this paper a general method of ϵ determination for each real sample from the function $\epsilon(E_\gamma)$ obtained for a calibration sample. The method takes into account the differences of density, and even of counting geometry, between the real and the calibration samples, because the soil samples studied have similar compositions [9]. It is based on the transmission method developed by Cutshall et al. [10] and modified by Joshi [11], and allow

*Corresponding author.

PII S0168-9002(96)00790-5

the direct determination of the full-energy peak efficiencies with relative uncertainties lower than 10%.

After presenting the detector and samples used in this work in Section 2 we describe the method in Section 3. Our results are validated in Section 4 and some conclusions close the paper in Section 5.

2. Experimental

The calibration procedure was developed for a conventional HPGe coaxial detector, 1.88 keV resolution and 14% relative efficiency linked to standard electronics and to a PC-based 4k multichannel analyzer. Measurements of low levels of radioactivity were possible by surrounding the detector with 10 cm thick lead shielding, internally lined with 2 mm of copper. A cylindrical container, 6.50 cm in diameter, was always used for sample counting, and placed on the top of the detector.

The soil selected for calibration was dried overnight at 105°C and subsequently powdered and homogenized. The other samples were prepared in an identical way.

A standard ^{152}Eu solution was used to determine efficiencies at calibration counting conditions. ^{152}Eu γ-emissions of low or poorly known emission probability [12] were rejected and so only ten γ-lines, covering an energy range from 120–1500 keV, were chosen to perform the efficiency calibration process. This is the energy range interesting for us and measurable by our conventional detector.

Thus, the soil calibration sample (apparent density ρ_c = 1.48 g cm^{-3}) was spiked with a well known ^{152}Eu activity. To assure perfect mixing of the spike in the soil matrix, several homogeneity tests were carried out measuring aliquots at the same conditions. As soon as homogeneity was confirmed we proceeded to the calibration process.

3. The method

The set of full-energy peak efficiencies, ϵ_c, obtained for the calibration soil cannot be used in Eq. (1) to obtain A in a real soil sample. Instead, ϵ_s (set of efficiencies for the real sample) is needed which, according to Ref. [10], for a given counting geometry can be described as

$$\epsilon_s = f\epsilon_c \tag{2}$$

where f is the transmission factor which accounts for the self-absorption relative differences between the real sample and the calibration sample. In fact, f is defined as

$$f = S/C \tag{3}$$

with S and C being respectively the net count rates under the full-energy peak of interest produced by the same activity in the real and in the calibration soil samples.

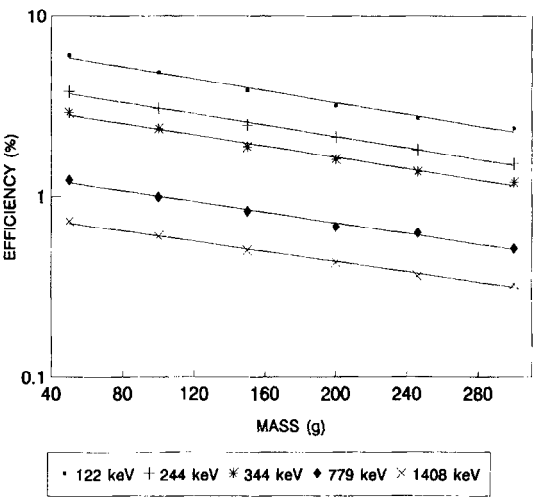

Fig. 1. Full-energy peak efficiency vs sample mass for different energies in the calibration sample.

When the counting geometry is cylindrical, as in our case, f can be determined experimentally by performing some photon transmission experiments [10,11]. Thus, if S_0 and C_0 are respectively the net count rates under the full-energy peak of interest obtained by counting a γ-emitting point source placed at the top of the real and calibration samples, f becomes

$$f = \frac{1 - S_0/C_0}{\ln(C_0/S_0)} = \frac{1 - e^{-(\mu_s - \mu_c)L}}{(\mu_s - \mu_c)L} \tag{4}$$

μ_s and μ_c are the linear attenuation coefficients for the real and calibration soil sample at the energy of interest, L is the cylinder height (or sample height).

It is clear that for a given sample height, L, f depends on the real sample density, ρ_s, and the photon energy, E_γ. So, f should be determined for each ρ_s and E_γ one is interested in Ref. [13]. For multi-elemental determinations this practice is time consuming. It is worthwhile, therefore, to find the functional dependence of f on ρ_s, E_γ and L.

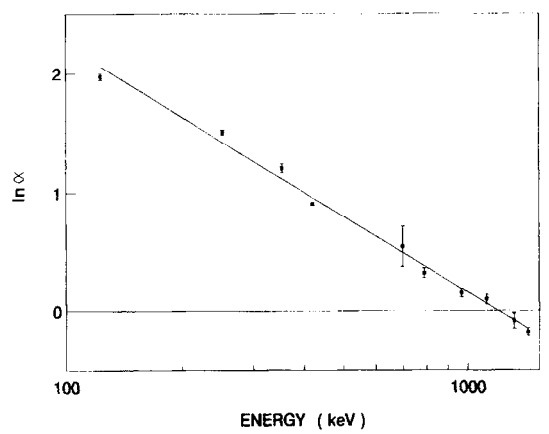

Fig. 2. Logarithm of parameter α of Eq. (5) vs γ-emission energy.

This will be tried in what follows. However, firstly we will determine the dependence of ϵ_c on E_γ and on L.

3.1. ϵ_c Determination

ϵ_c was determined for each ^{152}Eu γ-energy selected and for a wide range of L values, i.e. sample mass values, since the diameter of the cylinder is constant. In Fig. 1 we plot $\epsilon_c(\%)$ against calibration soil sample mass, M_c, for some E_γ values. For each energy it is found that

$$\epsilon_c = \alpha e^{-\beta M_c} = \alpha e^{-\beta \rho_c V_c} \tag{5}$$

where α and β are parameters which depend on E_γ, and ρ_c and V_c are the density and sample volume.

The meanings of α and β are clear. α is the full-energy peak efficiency for $L = 0$, that is, the efficiency function for a disk source of the same diameter as that of the cylinder at the position of the cylinder bottom. On the other hand, β or $\beta\rho_c$ gives the relative variation of ϵ_c per unit of added mass or volume.

In Fig. 2 and Fig. 3 we can see the dependence of α and β on E_γ. According to the above commented meaning of α and, as it has been previously found by other authors [14,15], α can be adequately described as a potential function of E_γ. This is confirmed by us, and we obtain

$$\ln\alpha[\%] = 6.44 - 0.909\ln(E_\gamma/E_0) \quad (\chi^2_R = 1.80) \tag{6}$$

where $E_0 = 1$ keV.

It is seen, on the other hand, that β is almost independent of E_γ, at least for $E_\gamma > 300$ keV, and slightly depends on the energy for smaller E_γ. Thus, the average value of β in the 300–1500 keV energy interval is

$$\langle\beta\rangle\rho_c = (4.87 \pm 0.10) \times 10^{-3}\ [\mathrm{cm}^{-3}] \tag{7}$$

Finally, ϵ_c becomes

$$\epsilon_c[\%] = 624 E_\gamma^{-0.909} \exp(-4.87 \times 10^{-3} V_c) \quad (\chi^2_R = 0.92) \tag{8}$$

where E_γ is expressed in keV and V_c in cm^3.

In deriving Eq. (8), the corrections due to true coincidence summing effects, related to cascade gamma emissions of ^{152}Eu were considered. These corrections were measured experimentally for the different geometries applying the method of Quintana and Fernandez [16], and are low (generally less than 10%, especially for the high volumes) as can be expected from the low relative efficiency of our coaxial detector (14%). We have also observed, that if these corrections are not considered, their effects are smoothed in the fittings, producing errors in the estimation of $\epsilon_c(\%)$ that range from 5% to 10%.

3.2. f Determination

The functional dependence of f on E_γ, ρ_s and L has been determined by performing transmission experiments through soil samples with apparent densities ranging from 0.6 to 1.7 g cm^{-3}. To achieve it, gamma emitting point sources of ^{226}Ra, ^{137}Cs and ^{60}Co were used and five heights (L = 1, 2, 3, 4 and 5 cm) explored. In this way a good range of ρ_s, L and E_γ was studied by using the counting geometry previously described.

As it can be seen in Fig. 4 and Fig. 5 the variation of f with ρ_s for a given E_γ and L can be described by

$$f = a e^{-b\rho_s} \tag{9}$$

where a and b are two parameters which depend on E_γ and L as it can be deduced from the data presented in Table 1. There we give the results of the fit according to Eq. (9).

It is easy to find the meanings of a and b. Indeed, μ_s

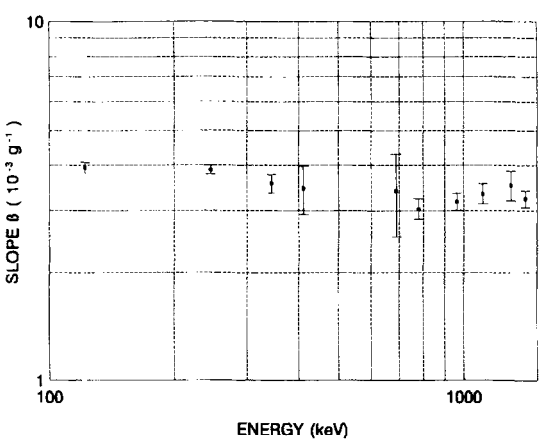

Fig. 3. Parameter β of Eq. (5) vs γ-emission energy.

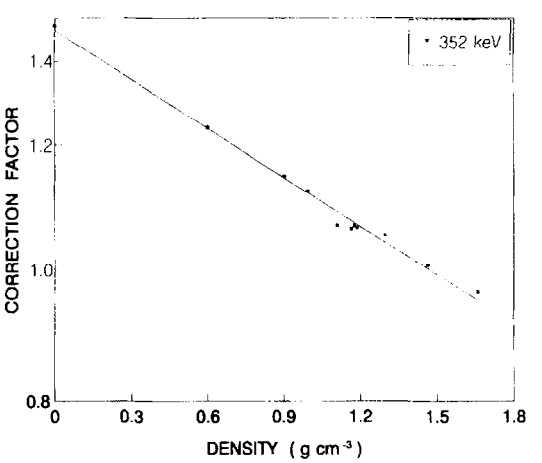

Fig. 4. Correction factor, f, vs apparent density of soil samples for E_γ = 352 keV and L = 5.0 cm.

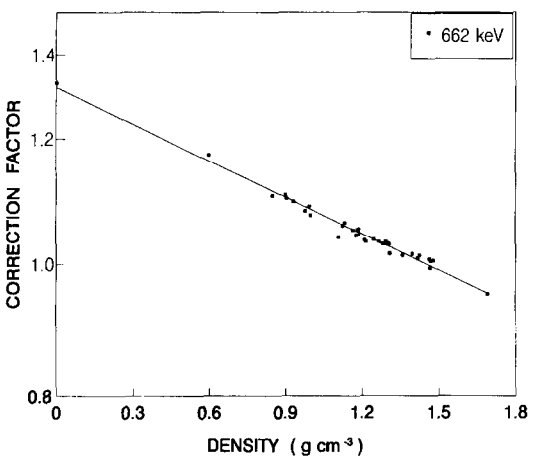

Fig. 5. Correction factor, f, vs apparent density of soil samples for $E_\gamma = 662$ keV and $L = 5.0$ cm.

and μ_c of Eq. (4) can be transformed into η_s and η_c being respectively the mass attenuation coefficients for the real and calibration samples. Thus we obtain

$$f = \frac{1 - e^{-(\eta_s\rho_s - \eta_c\rho_c)L}}{(\eta_s\rho_s - \eta_c\rho_c)L} = \frac{1 - e^{-x}}{x} \tag{10}$$

Obviously, $x = (\eta_s\rho_s - \eta_c\rho_c)L$. For $x \ll 1$ we obtain

$$f \approx 1 - \tfrac{1}{2}x \approx e^{-x/2} = e^{\eta_c\rho_c L/2} e^{-\eta_s\rho_s L/2} = a e^{-b\rho_s} \tag{11}$$

where $a = \exp(\eta_c\rho_c L/2)$ and $b = \eta_s L/2$. The value of f from Eq. (11) is approximately equal to that from Eq. (10), their differences being lower than 2% for $E_\gamma > 122$ keV. On the other hand, $a = e^{a'}$, being $a' = \eta_c\rho_c L/2$, can be approximated for our calibration sample by $1 + a'$, and we obtain

$$f = \left(1 + \frac{\eta_c\rho_c L}{2}\right) e^{-\eta_s\rho_s L/2} = (1 + a')e^{-b\rho_s} \tag{12}$$

where the differences between $a = e^{a'}$ and $1 + a'$ are less than 6% for $E_\gamma > 300$ keV. Obviously a' and b depend on E_γ as the mass attenuation coefficients do. For $E_\gamma > 100$ keV the relationship between η and E_γ is potential [17,18]. And this is what we observe in Fig. 6 for $L = 5$ cm. The same dependence is found for the other L values studied ($L = 1$, 2, 3 and 4 cm). On the other hand, also from their definitions, a' and b depend linearly on L.

With this in mind the following functional forms for a' and b can be guessed

$$a' = c' E_\gamma^{-d'}, \quad b = c E_\gamma^{-d} \tag{13}$$

Table 1
Experimental values obtained for the parameters a and b (g^{-1} cm^3) of Eq. (9), together with the reduced chi-squared χ^2_R, obtained applying the least-square fitting method, for every height and energy of interest. * = Value obtained for the parameter is not significant at 95% level

Energy [keV]	$L = 4.0$ cm			$L = 5.0$ cm		
	a	b	χ^2_R	a	b	χ^2_R
186.2	1.653	0.327	0.453	1.692	0.377	1.042
242.0	1.480	0.265	1.238	1.610	0.367	1.580
295.2	1.406	0.235	0.772	1.509	0.285	0.983
351.9	1.335	0.205	1.092	1.444	0.259	2.196
609.3	1.261	0.162	2.143	1.328	0.201	3.983
661.7	1.248	0.158	3.423	1.328	0.200	2.900
1120.	1.210	0.157	0.829	1.245	0.165	0.763
1175.	1.181	0.121	0.687	1.242	0.153	0.269
1333.	1.142	0.103	0.954	1.244	0.145	0.467
1764.	1.155	0.096	0.323	1.174	0.119	0.605
Energy [keV]	$L = 2.0$ cm			$L = 3.0$ cm		
	a	b	χ^2_R	a	b	χ^2_R
186.2	1.187	0.145	0.738	1.386	0.229	0.260
242.0	1.220	0.136	0.644	1.347	0.211	0.798
295.2	1.172	0.111	0.518	1.259	0.169	0.580
351.9	1.143	0.101	1.409	1.229	0.153	1.090
609.3	1.109	0.075	0.558	1.173	0.114	1.015
661.7	1.112	0.082	3.451	1.169	0.117	4.510
1120.	1.081	0.067	0.647	1.150	0.113	0.739
1175.	1.099	0.062	0.731	1.135	0.091	0.863
1333.	1.073	0.051	0.917	1.139	0.084	1.455
1764	1.063	0.052	0.540	1.149	0.081	1.056
Energy [keV]	$L = 1.0$ cm					
	a	b	χ^2_R			
186.2	1.136	0.088	1.136			
242.0	1.133	0.089	1.071			
295.2	1.067	0.052	0.626			
351.9	1.049	0.044	1.332			
609.3	1.048	0.032	0.609			
661.7	1.050	0.039	2.387			
1120	1.065*	0.038*	0.614			
1175	1.026*	0.027*	1.614			
1333	1.037*	0.027*	0.862			
1764.	1.009*	0.023*	0.838			

c' and c being two parameters which depend linearly on L, E_γ in keV, while d' and d are two constant quantities proper of the calibration process.

The data of Table 2 reveal that Eq. (13) was a good choice for fitting a' and b (derived from data in Table 1) to E_γ for different L. On the other hand, in Fig. 7 and Fig. 8 it is shown how c' and c increase linearly with increasing L values and how d' and d are basically constants for our L range.

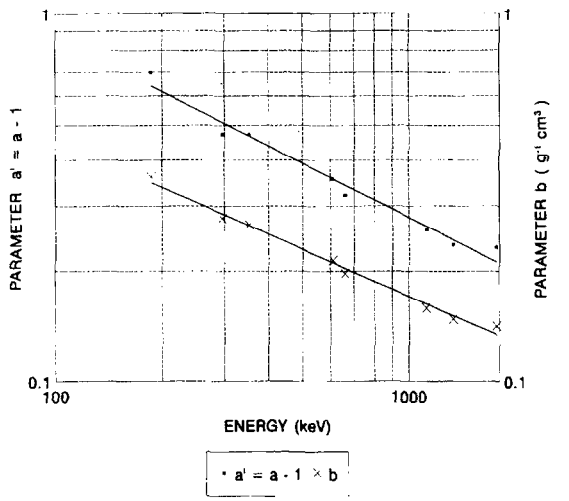

Fig. 6. Parameters $a' = a - 1$ and b (Eq. (9)) vs energy for the gamma emissions studied with $L = 5.0$ cm.

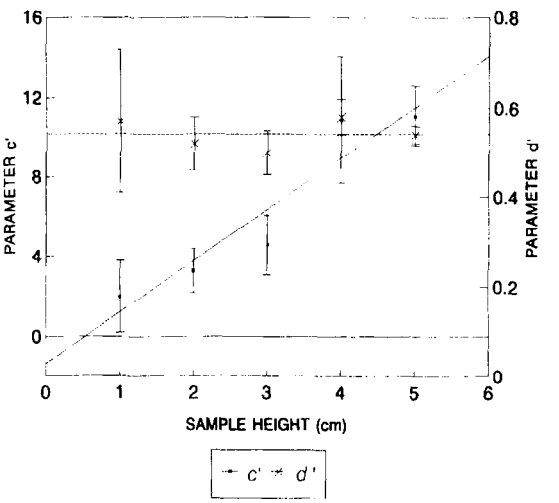

Fig. 7. Parameters c' and d' of Eq. (13) vs sample height (L).

Since L is proportional to V, that is proportional to M_s/ρ_s, c' and c can be simply expressed as functions of the type kM_s/ρ_s. By fitting the data in Fig. 7 and Fig. 8 to a linear function, it is found that

$$c = (0.04\pm0.28) + (0.0243\pm0.0028)\frac{M_s}{\rho_s}$$

$$c' = -(1.6\pm1.2) + (0.074\pm0.012)\frac{M_s}{\rho_s} \qquad (14)$$

where M is expressed in grams and ρ_s in g cm^{-3}.

On the other hand $d' = 0.543\pm0.015$ and $d = 0.485\pm0.021$ on the average. Thus, taking the average value of k for c and c'

$$a' = 0.0617E_\gamma^{-0.543}\frac{M_s}{\rho_s}, \quad b = 0.0243E_\gamma^{-0.485}\frac{M_s}{\rho_s} \qquad (15)$$

and, consequently

$$f = \left(1 + 0.0617E_\gamma^{-0.543}\frac{M_s}{\rho_s}\right)\exp(-0.0243E_\gamma^{-0.485}M_s) \qquad (16)$$

which is the functional dependence of f on E_γ, ρ_s and M (or L) we were looking for.

Table 2
Values obtained for the parameters c', d', c, d (Eq. (13)) and the reduced chi-squareds χ^2_R, obtained applying the least-square fitting method, for each height considered. * = Value obtained for the parameter is not significant at 95% level

V [cm^3]	L [cm]	c'	d'	χ^2_r
33.7	1.0	2.0±2.0*	0.57±0.16	2.24
67.4	2.0	3.3±1.1	0.52±0.06	1.008
101	3.0	4.6±1.5	0.50±0.05	1.858
135	4.0	10.9±3.2	0.58±0.05	1.113
168	5.0	11.1±1.5	0.54±0.02	1.127
V [cm^3]	L [cm]	c [g^{-1}cm^3]	d	χ^2_r
33.7	1.0	1.48±1.0*	0.57±0.11	0.835
67.4	2.0	1.55±0.35*	0.46±0.04	1.150
101	3.0	2.40±0.50	0.46±0.04	1.010
135	4.0	3.25±0.90	0.46±0.04	1.605
168	5.0	4.22±0.50	0.47±0.02	1.251

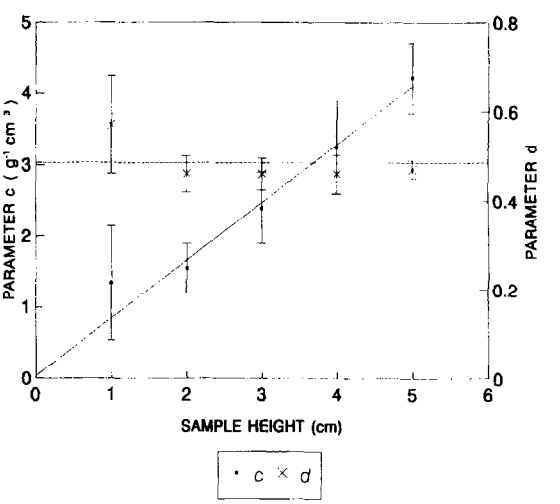

Fig. 8. Parameters c and d of Eq. (13) vs sample height (L).

Table 3
Average specific activities determined in an intercomparison exercise, and in our laboratory, measuring a marine sediment prepared by CIEMAT

Radionuclide	Energy [keV]	Specific activity of our laboratory [Bq/kg]	Average specific activity of the intercomparison [Bq/kg]
^{214}Pb	295.2	79.4±4.3	74.0±8.0
^{214}Pb	351.9	77.5±4.0	74.9±10.2
^{214}Bi	609.3	66.2±3.4	69.5±8.4
^{214}Bi	1764.5	77.1±4.4	74.7±9.7
^{212}Bi	300	42.2±4.0	43.5±7.4
^{228}Ac	911	36.9±2.2	39.5±4.2
^{137}Cs	661.7	12.1±0.7	12.9±1.3
^{40}K	1460.8	1413±70	1480±170

The uncertainty of f is expected not to exceed 6% even in unfavourable cases and may be as low as 1% for energies higher than 300 keV and density differences up to 0.5 g cm^{-3}.

By substituting Eq. (16) in Eq. (2) we have the general efficiency calibration equation for our measurement technique.

4. Validation tests

The validity of Eq. (2) and Eq. (16) has been tested by performing some tests. We present here the results obtained for a few of them.

In Table 3 we present the activities measured for a marine sediment distributed by the Spanish CIEMAT (Centro de Investigaciones Energéticas, Medio Ambientales y Tecnológicas) among a good number of Spanish environmental radioactivity laboratories. The sediment was counted in our geometry and had an apparent density of 1.66 g cm^{-3}. By applying Eq. (16) and Eq. (2) we obtained the results presented in column 3 of Table 3. In the column 4 of the same Table the average specific activities calculated in the intercomparison exercise are given. It is obvious that our results agree very well with them within the quoted 1σ uncertainties.

The results of Table 3 provide an additional validation test. As it should be expected we found, within the uncertainty limits, the same specific activity for those radionuclides which are expected to be in secular equilibrium, e.g. for the pair ^{214}Pb–^{214}Bi. Since their activities were calculated by using different E_γ, this simple exercise served us to see the validity of Eq. (16) within a wide energy range.

In Table 4 we compare the ^{228}Th activities obtained in different sediments by using our γ-spectrometry method and the traditional α-spectrometry method. ^{228}Th was determined both by measuring the 583 keV γ-emission from ^{208}Tl and the 911 keV γ-emission from ^{228}Ac(^{228}Ra). This exercise was done for several soils with different densities, ρ_s, and the counting performed under our cylindrical geometry with $L = 5.0$ cm. The results show a general noticeable agreement between α-spectrometric and both γ-spectrometric determinations. This confirms the goodness of our approach. The exceptions are samples SOT5 and SOT7 for which the agreement is not so obvious. For these cases, however, α-spectrometry determinations are compatible with ^{228}Ac measurements within 2σ. The reason for such disagreement is not clear.

Table 4
Results of measurements done in sediment samples from South of Spain. ^{228}Th and ^{228}Ra specific activities were determined by γ-ray spectrometry and also ^{228}Th by α-spectrometry.

Sample	Density [g cm^{-3}]	^{228}Th(^{208}Tl) (583 keV)	^{228}Th α-spectrometry	^{228}Ra(^{228}Ac) (911 keV)
SOT1	1.57	20.3±1.4	19.0±1.1	19.9±1.7
SOT2	0.98	64.1±3.6	64.6±3.1	58.1±3.8
SOT3	1.69	21.6±1.5	19.3±1.3	20.7±1.7
SOT4	1.09	39.3±2.8	40.9±2.4	46.7±3.6
SOT5	0.96	38.2±2.5	52.0±2.8	40.2±3.2
SOT6	0.94	64.3±3.6	65.8±3.7	58.1±4.0
SOT7	0.89	49.6±3.1	61.9±3.1	50.6±3.8
SOT8	1.00	44.8±2.8	43.0±2.3	43.2±3.2
SDR1	0.76	61.8±3.6	62.1±3.1	60.9±4.3
SDR2	0.93	41.8±2.5	34.9±2.6	43.0±2.8
SDR3	0.90	36.8±2.4	34.2±1.9	39.8±3.0
SDR4	1.02	37.6±2.2	34.8±5.7	40.1±2.8

Table 5
Fittings obtained for Eq. (17), applying the least-square method, for every energy considered

Nuclide	Energy [keV]	P_γ [%]	N_0 [cps/30 g]	$\rho\beta$ [10^{-3}cm^{-3}]
^{226}Ra + ^{235}U	186.2	3.51 + 57.2	2.320±0.024	6.34±0.12
^{214}Pb	295.2	18.2	1.346±0.033	5.79±0.29
^{214}Pb	351.9	35.1	1.177±0.014	5.74±0.14
^{214}Bi	609.3	44.6	0.600±0.008	5.44±0.08
^{214}Bi	1120.3	14.7	0.331±0.005	5.02±0.18
^{214}Bi	1764.5	15.1	0.236±0.009	4.99±0.40

Not obvious analytical errors in the α-spectrometric determinations cannot be excluded [19]. Nevertheless, the goodness of our method is apparent if one observes the whole set of results.

Finally, we have performed an additional exercise to check the validity of Eq. (5) and the assumption of β being a constant.

For that, a powdered phosphate rock sample ($\rho = 1.54$ g cm^{-3}) was used. This sample contained high radioactivity concentrations of U [^{238}U] of about 1200 Bq/kg, and daughters. It allowed a more precise determination of the parameter β.

Different amounts of the sample (M and, consequently, L or V) were measured in our cylindrical geometry. According to Eq. (1), ϵ is proportional to $N = n/(MP_\gamma)$, where n is the net count rate under full-energy peak of interest in counts/s. Consequently, if Eq. (5) is correct it should be

$$N = N_0 e^{-\beta\rho V} \tag{17}$$

This function was fitted for each energy considered in our exercise to the experimental values obtained for the difference sample amounts. The N_0 and $\rho\beta$ values are given in Table 5. The fitting was very satisfactory with values of χ^2_R close to unity.

And, as it was expected, N_0 depends on E_γ as α does (see Fig. 9). However, the parameter β (or $\rho\beta$) shows a slight dependence on E_γ as it is observed in Fig. 9. This is demonstrating that, as expected, the effect of self-absorption on β is detectable when the accuracy of measurements is improved. However, the maximum difference between $\rho\beta$ obtained from Eq. (7) and the average of $\rho\beta$ from Table 5 (Fig. 9) is only around 6%. This means that the use of Eq. (7) is essentially correct for our purposes.

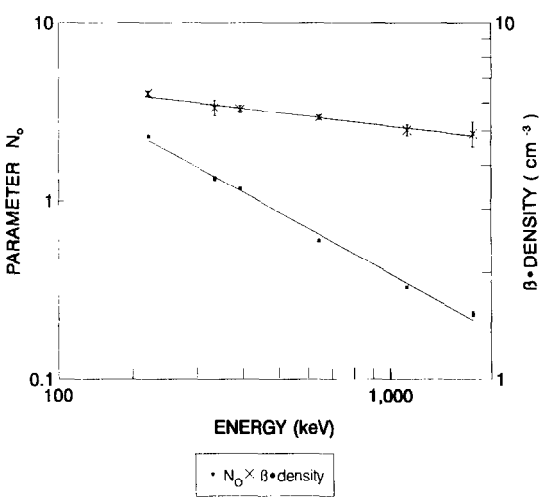

Fig. 9. Plot of the parameter N_0 and β (Eq. (17)) vs γ-ray energy for the gamma emissions studied.

5. Conclusions

A general method for γ-ray efficiency calibration of Ge coaxial detectors is presented. It is based on the transmission method and, in fact, is a generalization of such procedure. The transmission factor, f, is described as a single function of E_γ, sample density and geometry. Although the method has been developed for soil samples, its underlying philosophy makes it useful for any sample for which the measuring geometry can be adequately reproduced.

Acknowledgments

This work has been partially supported by ENRESA, the U.E. project F13-P-CT92-0035 and the project of Junta de Andalucia "Estudio de los flujos de radionúclidos en la producción de pasta de papel y su aplicación en la optimización del proceso industrial".

References

[1] F. El-Daoushy and R. Garcia-Tenorio, Nucl. Instr. and Meth. A 356 (1995) 376.
[2] P.G. Appleby, P.J. Nolan, F. Oldfield, N. Richardson and S.R. Higgit, Sci. Tot. Environ. 69 (1988) 157.
[3] M.E. Kitto, Int. J. Appl. Instr. Part A 42 (1991) 835.
[4] E. Cincu, Nucl. Instr. and Meth. A 312 (1992) 226.
[5] R.S. Seymour, M.S. Andreaco and J. Pierce, J. Radioanal. Nucl. Chem. Art. 123 (1988) 529.

[6] G. Harbottle, Radioact. and Radiochem. 4 (1993) 20.
[7] A.S. Murray, R. Marten, A. Johmston and P. Martini, J. Radioanal. Nucl. Chem., Art. 115 (1987) 263.
[8] M.E. Kitto, J. Radioanal. Nucl. Chem. Lett. 145 (1990) 175.
[9] J.E. Martin, J.P. Bolivar, M.A. Respaldiza, R. Garcia-Tenorio and M.F. da Silva, Nucl. Instr. and Meth. B 103 (1995) 477.
[10] N.H. Cutshall, I.L. Larsen and C.R. Olsen, Nucl. Instr. and Meth. 206 (1983) 309.
[11] S.R. Joshi, Appl. Radiat. Isot. 40 (1989) 691.
[12] D.C. Kocher, Radioactive Decay Data Tables (D.O.E., T.I.C.-11026, Springfield, 1984).
[13] S.R. Joshi, J. Radioanal. Nucl. Chem. Articles 116 (1987) 169.
[14] C.I. Sánchez, R. García-Tenorio, M. García-León, J.M. Abril and F. El-Daoushy, Nucl. Geophys. 6 (1992) 395.
[15] A.F. Sánchez-Reyes, M.I. Febrián, J. Baró and J. Tejada, Nucl. Instr. and Meth. B 28 (1987) 123.
[16] B. Quintana and F. Fernandez, Appl. Radiat. Isot. 48 (1995) 961.
[17] J.M. Hubbell, Int. J. Appl. Radiat. and Isot. 33 (1982) 1269.
[18] K. Debertin and R.G. Helmer, Gamma and X-Ray Spectrometry with Semiconductor Detectors (North-Holland, Amsterdam, 1988).
[19] J.P. Bolivar, Aplicaciones de las Espectrometrías Alfa y Gamma al Estudio del Impacto Radiactivo Producido por Industrias No Nucleares, Ph. Thesis (Universidad de Sevilla, Sevilla, 1995) in Spanish.